Quantum Spintronics: A Sub-Landauer-Bound Computing Paradigm

Frank Z. Wang

Division of Computing, Engineering & Mathematics Sciences, University of Kent, Canterbury, CT2 7NF, the UK (f.z.wang@kent.ac.uk)

ABSTRACT A quantum electronic device stimulates the interaction of coherent electromagnetic radiation (typically with submillimetre wavelengths) on the quantum level. In this study, we compared two typical spintronic systems in terms of using spins as qubits: one is a giant spin (molecular nanomagnet) with strong anisotropy due to the spin-lattice coupling; the other is a single spin that is weakly bound in an ion. We found that, although both use quantum spin tunnelling, the single spin is much more 'agile' than the giant spin (whose 'clumsiness' is not only due to its 'giant' size but also due to its strong coupling with the surroundings) and can break Landauer's bound (the energy of erasing a classical bit of information) by a factor of $10^4 \sim 10^{10}$. Experimental verification is provided, in which the single spin is optically manipulated by a circularly polarized on-resonant laser (with a wavelength ranging from 422 nm to 1092 nm) and Rabi flopping at mHz. In conclusion, quantum spintronics (with a single spin as a qubit) may represent a new energy-efficient computing paradigm within the context that the increase in the computing power efficiency will come to a halt around 2050 due to Landauer's bound.

INDEX TERMS quantum spin electronics (spintronics), submillimetre wavelength, Rabi frequency, qubit, Landauer's bound, quantum spin tunnelling, adiabatic quantum computer.

I. Introduction

The physical implementation of two-level quantum systems (qubits) matters in terms of building a working device. A quantum electronic device stimulates the interaction of coherent electromagnetic radiation (typically with a wavelength in the submillimetre range) on the quantum level and the transition between quantum energy levels.

Qubits have served as quantum counterparts to classical bits since the 1990s. As the unit of a classical computer, a classical bit can only take either the '0' or '1' state. To describe a classical bit sharply switching between '0' and '1', one must make some approximations to the initial Hamilton's equation (or its counterpart for an electric system). This is because, characterized by its position and momentum, a classical object can only take a value within a continuous range and continuously change with time [1].

A quantum state of a qubit with mutually orthogonal unit vectors $|0\rangle$ and $|1\rangle$ can be written as $|\Psi\rangle = \alpha |0\rangle + \beta |1\rangle$, where complex numbers α and β satisfy the condition $|\alpha|^2$ + $|\beta|^2 = 1$ ($|\alpha|^2$ is the probability of finding the qubit in $|0\rangle$, and $|\beta|^2$ is the probability of finding the qubit in $|1\rangle$). To find a quantum system in a certain state, we need some physical quantities (observables). By measuring one of the observables many times, we will obtain the probability of finding the system in the corresponding state on average [1].

To date, many kinds of qubits have been successfully fabricated. One kind is charge qubits that use quantum dots (Figure 1). Such a dot is so small that it can contain no more than one electron at a given time since electrons with the same electric charge strongly repel each other. By putting one electron across two neighbouring quantum dots, we can actually obtain a charge qubit. The states $|0\rangle$ and $|1\rangle$ can be detected by measuring the local electric potential, and the electron can be moved around by applying a voltage with an approximate value [2].

If the dot (island) is made of a superconductor, then we obtain a superconducting charge qubit [Figure 2(a)], where |0\rangle and |1\rangle represent the presence or absence of a Cooper pair [3] or BCS pair of electrons, respectively.

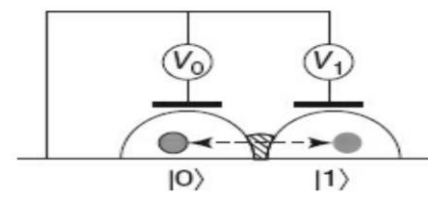
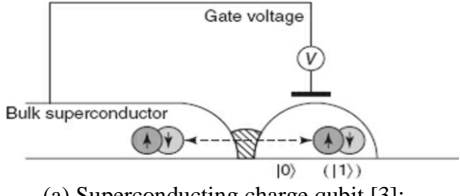
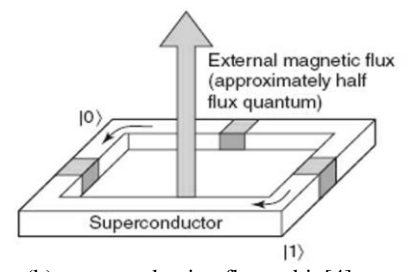


Figure 1. Charge qubit comprising two quantum dots [2].

Due to its special property (a superconducting loop can carry an electric current forever), the usage of a superconductor in a qubit makes it possible to protect its state from external noise. By interrupting a superconducting loop with a Josephson junction [4], we obtain a superconducting flux qubit ('flux' refers to the magnetic flux, produced by the current flow), as shown in Figure 2(b). The states $|0\rangle$ and $|1\rangle$ represent the counterclockwise current flow and the clockwise current flow, respectively.



(a) Superconducting charge qubit [3];



(b) superconducting flux qubit [4].

Figure 2. Superconducting qubit [3][4].

It is worth mentioning that the electric charge in the above charge qubit consists of one or two electrons [2][3] whereas the current flow in the above flux qubit involves (typically) more than two electrons [4]. Nevertheless, these qubits still behave like two-level quantum systems.

II. Spintronics For Quantum Computing

In addition to the above discussed charge and flux qubits in conventional quantum electronics, another kind of qubit is the qubit based on spin, which is the angular momentum of a quantum particle, measured in units of \hbar : $L = \hbar s$ [5]. As an indispensable and inescapable property, the spin angular momentum cannot be reduced to zero or anything else. If a quantum particle as an information carrier is 'at rest' or 'anchored' (i.e., its kinetic energy has the minimal value allowed by Heisenberg's uncertainty principle [5]), then its spin is still present and can be manipulated and recorded. Scalably, the magnetic moment of a macroscopic particle consists of an integer number of spins. Such a macroscopic particle can also be manipulated by an external electromagnetic field. Being a quantum observable, spin is quantized such that s can be either an integer or a halfinteger: $s = \frac{1}{2}, \frac{3}{2}, \dots$ In particular, an electron, a proton or a neutron has spin-1/2 [5].

If a 'resting' electron is trapped or anchored in a potential well, then its two spin states can play the role of a qubit. As shown in Figure 3, the difference in energy between the two states '0' (when the magnetic moment is parallel to the magnetic field *B*) and '1' (when it is antiparallel) is $\Delta E_{\uparrow\downarrow} = \mu_B B$.

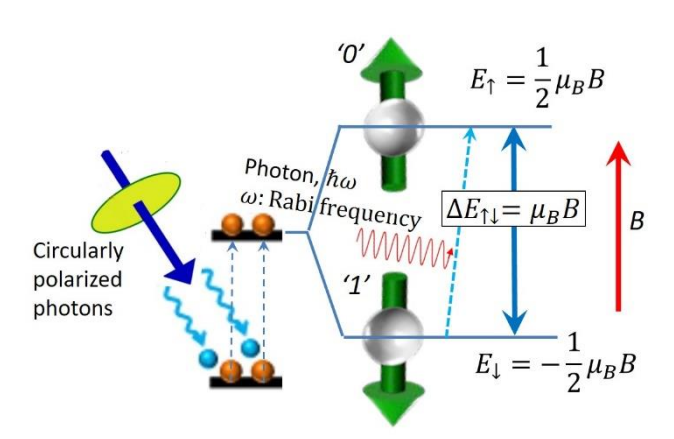


Figure 3. Energies of a spin qubit in a magnetic field B. A circularly polarized on-resonant μm laser cyclically pumps the spin qubit to a defined quantum state, followed by spin reversal induced by B. Rabi flopping between the two levels illuminated with light exactly resonant with the transition occurs at the Rabi frequency.

The spin-related magnetic dipole moment of an electron is $\mu_B = 9.2740 \times 10^{-24} J/T$ (the Bohr magneton [5]), that is, very small. For a proton, it is one nuclear magneton [5], $\mu_N = 5.0507 \times 10^{-27} J/T$, that is, even smaller. Nevertheless, the weakness of the signal of each spin does not stop us from using spins as qubits.

One method is to use multiple identical molecules, each containing several atoms with nuclear spin-1/2 (Figure 4) – e.g. 1H , ^{13}C or ^{19}F [6]. These spins interact with each other and can be controlled and measured using the nuclear magnetic resonance (NMR) technique. The large number of spins involved compensates for the weakness of the signal of each spin.

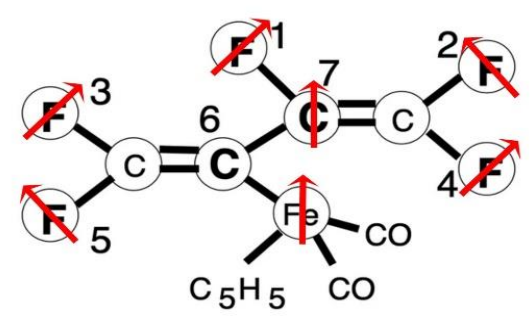


Figure 4. In 2001, an NMR quantum computer containing seven qubits (extracted from some atoms in a molecule) performed a real quantum algorithm (factoring the number $15 = 3 \times 5$) [6].

In 2014, a spin-spin magnetic interaction experiment [7] was carried out. A circularly polarized on-resonant laser (with a wavelength ranging from 422 nm to 1092 nm) cyclically pumped two electrons bound within two ions across a separation ($d=2.18\sim2.76~\mu m$) to a well-defined quantum state $|\uparrow\downarrow\rangle$ or $|\downarrow\uparrow\rangle$. The measured magnetic interaction was extremely weak $[B=\frac{\mu_0}{4\pi}\frac{2\mu_B}{d^3}=(0.88\sim1.79)\times10^{-13}~T$, where $\mu_0=4\pi\times10^{-7}T\cdot m/A$ is the vacuum permeability constant], six orders of magnitude smaller than magnetic noise (typically $0.1~\mu T$). As shown in Figure 5, the two ions were entangled to protect the two (entangled) spins against errors (decoherence processes). Relevant to our study here, a single spin can be reliably switched with a typical detection fidelity of 98% [7].

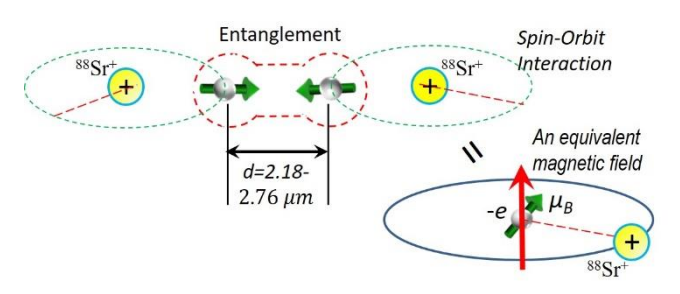


Figure 5. In 2014, the magnetic interaction between two outermost ground-state spin-1/2 valence electrons orbiting around two ⁸⁸Sr+ ions was measured [7]. The spin-spin interaction induces spin rotation since, as the smallest magnet (the Bohr magneton), a spin $(1 \mu_B)$ applies a tiny magnetic field to another spin. Due to the spin-orbit coupling, an equivalent (weak) magnetic field acts on each electron in its rest frame.

In 2018, a giant spin reversal experiment [8] was reported, in which each nanomagnetic bit was composed of eight spin-

 $\frac{5}{2}$ F_e^{3+} ions. These ions are coupled to each other by ferromagnetic interactions. A collective ($\frac{5}{2} \times 8 = 20 \,\mu_B$) giant spin is formed. With aligned magnetic axes, arrays of these molecular magnets can be packed into a single crystal (Figure 6, top). The Hamiltonian of this giant spin is

$$\mathcal{H} = -D_{ani}S_z^2 + E_{ani}(S_x^2 - S_y^2) - 2\mu_B \mathbf{S} \cdot \mathbf{B},\tag{1}$$

in which the first two terms account for the magnetic anisotropy energy involving the two anisotropy constants (D_{ani} and E_{ani}), and the third (Zeeman) term accounts for the interaction between the total spin S and a magnetic field B [8]. As shown in Figure 6 (bottom), an effective energy barrier was accordingly created, separating the $S_z = \pm 10$ ground eigenstates that encode the ' \uparrow ' and ' \downarrow ' bit states.

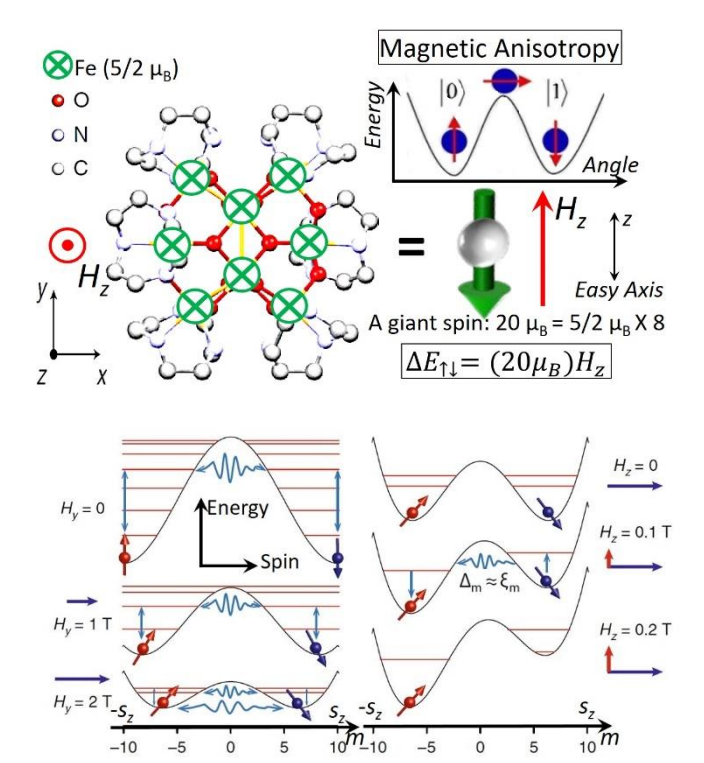


Figure 6. In 2018, a giant spin S_z = ± 10 (20 μ_B) reversal experiment was reported [8]. Here, x, y and z are defined as the hard, medium and easy magnetic axes, respectively. The (strong) magnetic anisotropy of spin-lattice relaxation is illustrated.

In this giant spin reversal experiment, two external magnetic fields (H_y, H_z) provide external control over the potential energy landscape. $H_y = (0 \sim 2) T$, is applied along the medium axis, allowing one to tune the height of the potential energy barrier without breaking the degeneracy between ' \uparrow ' and ' \downarrow '. This transverse magnetic field promotes quantum mixing of the ' \uparrow ' and ' \downarrow ' spin orientations in this quantum system [8]. The giant spin can then tunnel through the barrier via progressively lower-lying energy levels, thus leading to spin reversal (Figure 6, bottom left). In contrast, the other magnetic field $H_z = (0 \sim 0.2) T$, parallel to the easy

It is worth highlighting here that, compared to the weak magnetic interaction ($\sim 10^{-13} T$) in the previous spin-spin experiment [7], the strength ($\sim 0.1 T$) of the horizontal magnetic field H_z required to flip this (20 μ_B) giant spin is inevitably large to overcome the strong magnetic anisotropy in the crystal lattice structure (see details in Section IV).

Figure 6 (bottom) vividly illustrates spin relaxation combining tunnelling with spin-phonon coupling. Spin reversal occurs by the system absorbing a phonon (or a few phonons) in the excitation and reaching an excited state $(\Delta_m \approx \varepsilon_m)$, the spin tunnelling to the opposite side of the potential barrier, the system emitting a phonon (or a few phonons) in the de-excitation and eventually reaching the ground state. The above process may take a long relaxation time (>100 s), which can be improved by increasing H_y to lower the energy level so that $\Delta_m \gg \varepsilon_m$ [8].

There are two sides to everything. One problem with using multiple spins is their 'bulk' feature (all spins have to be controlled and measured at once) [1]. Another problem is that the strong coupling required to form a collective spin may result in disruption (from the environment) of the fragile quantum correlations essential for qubits [1]. A third problem is that some systems such as molecular nanomagnets exhibit a strong magnetic anisotropy that requires strong magnetic fields to drive them.

III. Spin Qubit Hamiltonian and Schrödinger Equation

The Hamiltonian of a spin qubit can be written in the Hermitian form with a special kind of symmetry (its diagonal elements being real and off-diagonal elements being complex conjugates) [1][5] as follows:

$$\hat{H} = -\frac{1}{2} \begin{pmatrix} \varepsilon & \Delta \\ \Delta & -\epsilon \end{pmatrix},\tag{2}$$

where ε is the bias (shown in Figure 7), and Δ is the tunnelling splitting (to be shown in Figure 8).

Consider a ball that is rolling on an uneven surface [Figure 7(a)] and will eventually settle in one of the local minima, with the minimum potential energy $E_{min} = mh_{min}$ (m denotes the mass of the ball, and h denotes the height of the ball). If two such minima are separated by a hill (an energy barrier), forming a two-well potential, then we can consider one of the two wells as '0' and the other as '1'. That is, the ball is our information carrier in a classical information system and its position is encoded as a binary bit of information. We may also assume that friction eventually stops the ball such that we can neglect its kinetic energy in this case (for a similar reason, we should use bound rather than free electrons while implementing quantum computing in spintronics). As shown in Figure 7(a), we can also create an energy difference ε between the two states: $\varepsilon = E_1 - E_0$.

Once the ball is in '0', it will stay there forever, even if $E_1 < E_0$. To force the ball to move from '0' to '1', we have

to push it over the hill (that is, Landauer's bound [9] in a classical information system; see the details in Section IV) by providing sufficient kinetic energy.

If the setup in Figure 7(a) is used for quantum computing (the ball is small enough and the barrier is narrow enough), then the ball can tunnel through the barrier with a rate Γ , as shown in Figure 7(b) [it can be considered as the quantum analogue of Figure 7(a)]. In theory, this tunnelling process does not require any extra energy and resembles teleportation [1].

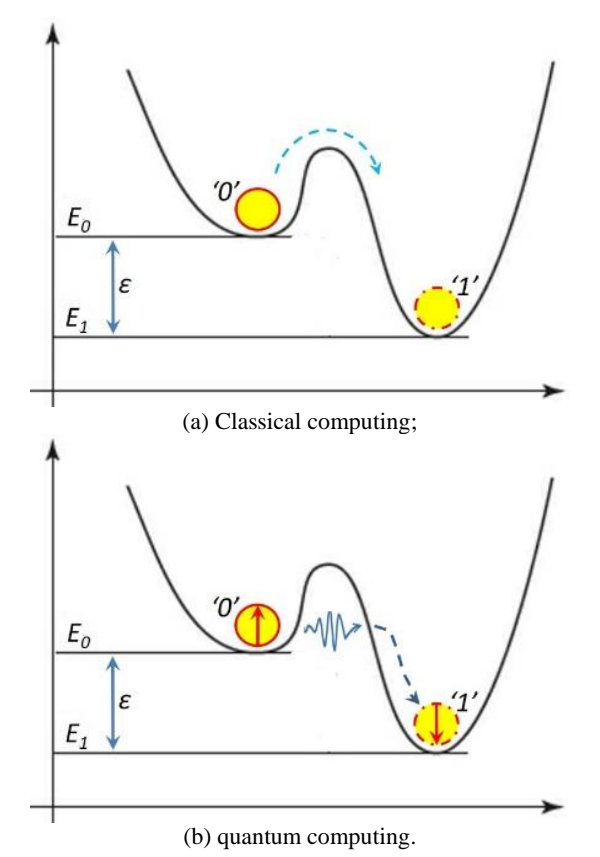


Figure 7. The two-well potential is used in both classical computing and quantum computing. If the ball is small enough and the barrier is narrow enough, then the ball can tunnel through the hill with no need to climb it.

The spin qubit Hamiltonian in the Schrödinger equation is

$$i\hbar \frac{d}{dt} {\alpha \choose \beta} = -\frac{1}{2} {\epsilon \choose \Delta} \frac{\Delta}{-\epsilon} {\alpha \choose \beta} = {-\frac{1}{2} \epsilon \alpha - \frac{1}{2} \Delta \beta \choose -\frac{1}{2} \Delta \alpha - \frac{1}{2} \epsilon \beta}, \quad (3)$$

where the 'energy' $\Delta \sim \hbar \Gamma$ (the frequency times the Planck constant yields the energy) is the tunnelling matrix element of the Hamiltonian [1].

This matrix equation is decomposed into a set of two equations: one corresponds the first row, and the other to the second row. If the qubit is not biased ($\varepsilon = 0$), then we obtain

$$i\hbar\frac{d\alpha}{dt} = -\frac{1}{2}\Delta\beta; i\hbar\frac{d\beta}{dt} = -\frac{1}{2}\Delta\alpha, \tag{4}$$

$$\frac{d\alpha}{dt} = \frac{i\Delta}{2\hbar}\beta; \frac{d\beta}{dt} = \frac{i\Delta}{2\hbar}\alpha. \tag{5}$$

Let us start from the state $|0\rangle$ ($\alpha=1,\beta=0$). We obtain $\frac{d\alpha}{dt}=0$ and $\frac{d\beta}{dt}=\frac{i\Delta}{2\hbar}$, which means that the chance of finding our system in state $|1\rangle$ changes at a rate $\Gamma\sim\frac{\Delta}{\hbar}$.

For a qubit, a solution (an energy eigenstate) in the form of $|\Psi_E\rangle = {\alpha \choose \beta} exp\left(-\frac{iEt}{\hbar}\right)$ satisfies the stationary Schrödinger equation:

$$-\frac{1}{2} \begin{pmatrix} \varepsilon & \Delta \\ \Lambda & -\varepsilon \end{pmatrix} \begin{pmatrix} \alpha \\ \beta \end{pmatrix} = E \begin{pmatrix} \alpha \\ \beta \end{pmatrix}, \tag{6}$$

where E is a definite energy [1].

These two equations for two unknown quantities can be resolved only if

$$E = \pm \frac{1}{2} \sqrt{\varepsilon^2 + \Delta^2},\tag{7}$$

in which the lower sign corresponds to the energy E_g of the ground state $|\Psi_g\rangle$ and the upper sign to the energy E_e of the excited state $|\Psi_e\rangle$, as shown in Figure 8.

From the above equations, we obtain that

$$\begin{split} \left|\Psi_g(\infty)\right\rangle &= \begin{pmatrix} 1\\0 \end{pmatrix} \text{ and } \left|\Psi_e(\infty)\right\rangle = \begin{pmatrix} 0\\1 \end{pmatrix}, \text{ when } \varepsilon \to \infty; \\ \left|\Psi_g(-\infty)\right\rangle &= \begin{pmatrix} 0\\1 \end{pmatrix} \text{ and } \left|\Psi_g(-\infty)\right\rangle = \begin{pmatrix} 1\\0 \end{pmatrix}, \text{ when } \varepsilon \to -\infty; \\ \text{and } \left|\Psi_g(0)\right\rangle &= \frac{1}{\sqrt{2}} \left[\begin{pmatrix} 1\\0 \end{pmatrix} + \begin{pmatrix} 0\\1 \end{pmatrix}\right] \text{ and } \\ \left|\Psi_e(0)\right\rangle &= \frac{1}{\sqrt{2}} \left[\begin{pmatrix} 1\\0 \end{pmatrix} - \begin{pmatrix} 0\\1 \end{pmatrix}\right], \text{ when } \varepsilon = 0. \end{split}$$

The above relations imply that a large bias ε (when the two wells are far apart) results in the state of the system being in either of the two wells [1], as shown in Figure 8.

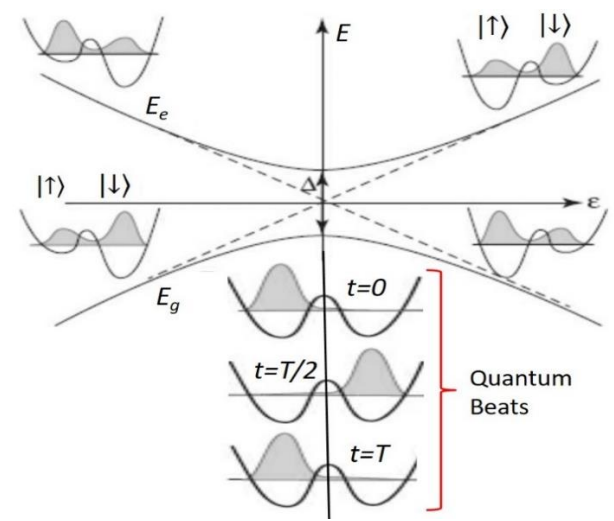


Figure 8. Energies and wavefunctions of the ground and excited spin qubit states. Quantum beats can be seen when $\varepsilon = 0$.

At zero bias ($\varepsilon=0$), the energies of the two wells coincide, but the energy gap between the ground and excited states is Δ (the tunnelling splitting). The eigenstates are superpositions of the ' \uparrow ' and ' \downarrow ' states: $|\Psi_g(0,t)\rangle=\frac{1}{\sqrt{2}}[|\uparrow\rangle+|\downarrow\rangle]exp\left(\frac{i\Delta t}{2\hbar}\right)$ and $|\Psi_e(0,t)\rangle=\frac{1}{\sqrt{2}}[|\uparrow\rangle-|\downarrow\rangle]exp\left(-\frac{i\Delta t}{2\hbar}\right)$.

If the system is in state $|\uparrow\rangle$ at t=0, then it can be written as

$$\begin{split} |\uparrow\rangle &= \frac{1}{2} [(|\uparrow\rangle + |\downarrow\rangle) + (|\uparrow\rangle - |\downarrow\rangle)] = \frac{1}{2} \left[\sqrt{2} \left| \Psi_g(0, t = 0) \right\rangle + \sqrt{2} \left| \Psi_e(0, t = 0) \right\rangle \right]. \end{split} \tag{8}$$

To find the state of the system at any later time, we need to include the time-dependent vectors and obtain

$$\begin{split} |\Psi(t)\rangle &= \frac{1}{2} \left[\sqrt{2} |\Psi_{g}(0,t)\rangle + \sqrt{2} |\Psi_{e}(0,t)\rangle \right] \\ &= \frac{1}{2} \left[|\uparrow\rangle \left(e^{\frac{i\Delta t}{2\hbar}} + e^{-\frac{i\Delta t}{2\hbar}} \right) + |\downarrow\rangle \left(e^{\frac{i\Delta t}{2\hbar}} - e^{-\frac{i\Delta t}{2\hbar}} \right) \right] \\ &= \left[|\uparrow\rangle \cos\frac{\Delta t}{2\hbar} + i|\downarrow\rangle \sin\frac{\Delta t}{2\hbar} \right]. \end{split} \tag{9}$$

At time $t = \pi \hbar / \Delta t$, the system will be in the $|\downarrow\rangle$ state although we did nothing to it. It will keep oscillating between $|\uparrow\rangle$ and $|\downarrow\rangle$. The probabilities of finding the qubit in states $|\uparrow\rangle$ and $|\downarrow\rangle$ are

$$P_{\uparrow}(t) = |\alpha|^2 = |\langle \uparrow | \Psi(t) \rangle|^2 = \left(\cos \frac{\Delta t}{2\hbar}\right)^2 = \frac{1}{2} \left(1 + \cos \frac{\Delta t}{\hbar}\right)$$

$$P_{\downarrow}(t) = |\beta|^2 = |\langle\downarrow|\Psi(t)\rangle|^2 = \left(\sin\frac{\Delta t}{2\hbar}\right)^2 = \frac{1}{2}\left(1 - \cos\frac{\Delta t}{\hbar}\right),$$
respectively

This leads to a phenomenon called quantum beats [1][10] (Figure 8) and the period is $T = \frac{2\pi\hbar}{\Delta} = \frac{h}{\Delta}$. The above deductions vividly demonstrate that the quantum dynamics of a spin qubit are largely determined by its energy time product ($Et = \Delta T$) in terms of setting the maximum speed at which a spin can modify its energy by a given amount. Further elaborations will be provided in the following sections.

On the other hand, the tunnelling in the spin-flipping by a magnetic field is irreversible since the magnetic field only favours flipping a spin with the opposite direction. This magnetic field tilts the potential landscape such that $\varepsilon \neq 0$, as shown in both Figure 6 (bottom right) and Figure 7(b). Thus, a single spin can still be reliably switched without having the problem that the information carrier in the destination well 'tunnels' back to the original well in the completed erasure. Such reliable switch has been experimentally observed in both the spin-spin magnetic interaction experiment (with a typical detection fidelity of 98%) [7] and the (20 μ_B) giant spin reversal experiment [8].

IV. Landauer's Bound and Quantum Spin Tunnelling

If we take the strongest instantaneous magnetic field of 1,200 Tesla created in the laboratory [11] as B in Figure 3, then $\Delta E = \mu_B B \approx 10^{-18} J$. Table 1 lists the energies to flip a spin with different magnetic fields in comparison to Landauer's bound [9].

In Section II, we mentioned that, in contrast to the weak magnetic interaction $[(0.88 \sim 1.79) \times 10^{-13} \ T]$ in the spin-spin experiment [7], the strength $(\sim 0.1\ T)$ of the horizontal magnetic field required to flip the $(20\ \mu_B)$ giant spin is inevitably large to overcome the strong magnetic anisotropy in the crystal lattice structure [8]. As another comparison, the equivalent magnetic field (due to the spin-orbit coupling as shown in Figure 5) acting on the outermost electron orbiting around an 88 Sr+ ion in the rest frame of this electron is only $\frac{Z^4}{n^3} \approx 10^{-7}\ T$ [5], as listed in Table 1.

In Section III, we mentioned that the tunnelling process approximately does not require any extra energy. However, it is only theoretically possible to use zero or an arbitrarily small energy to flip a spin via tunnelling, whereas in practice this energy must have a lower bound. As listed in Table 1, the current world record is 10^{-36} J. This is analogous to the world record of the lowest temperature $(3.8 \times 10^{-11} \ K)$ [17], although in theory one can get as close as possible to absolute zero.

Table 1. Energies to flip a spin or a $(20 \,\mu_B)$ giant spin with different magnetic fields (sorted by amplitude from large to small) in comparison to Landauer's bound $(k_B \, \text{T ln 2})$ [9].

Scenario, in which a spin or a giant spin is placed.	Magnetic Field B	Energy ($\mu_B B$) to Flip a Spin in B	
Strongest magnetic field in the universe [11]	10° T	10 ⁻¹² /	
Strongest magnetic field in the lab [11]	1,200 T	10 J 10 ⁻¹⁸ J	
Strongest (steady) magnetic field in the lab [12]		$5 \times 10^{-20} J$	
Landauer's bound [9] at 300 K	n/a	$10^{-21} J$	
Magnetic resonance imaging (MRI) [13]	9.4 T	$10^{-22} J$	
(20 μ_B) giant spin reversal experiment at 1 K [8]	0.1 <i>T</i>	$1.855 \times 10^{-23} J$	
Landauer's bound [9] at 1 K	n/a	10 ⁻²³ J	
Transformer [14]	1 T	$10^{-23} J$	
Landauer's bound [9] at 1 mK	n/a	$10^{-26} J$	
Earth's magnetic field [15]	$10^{-5}T$	$10^{-28} J$	
Outermost electron orbiting around ⁸⁸ Sr+ in the spin-spin experiment [7]	$10^{-7} T$	$10^{-30} J$	
Outermost electron in a Rydberg atom (n=630) [5]	10 ⁻⁹ T	$10^{-32} J$	
Brain magnetic field [15]	1 pT	$10^{-35} J$	
Spin-spin magnetic interaction at 1 <i>mK</i> [7][16]	$10^{-13} T$	$10^{-36} J$	

The so-called Landauer's bound was proposed by Rolf Landauer in 1961 [9], who argued that information is physical and that the erasure of a bit of classical information requires a minimum energy amounting to $\Delta E = k_B T \ln 2$, where k_B is the Boltzmann constant and T is the temperature. Profoundly, Landauer's bound (Figure 9) is accepted as one of the fundamental limits in physics and computer science [18].

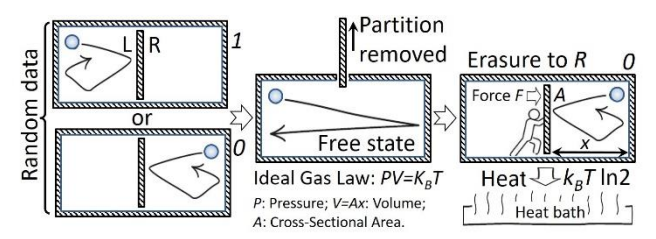


Figure 9. For a bit of position-encoded classical information, the designated erasure state ("0") is reached from the random data state via the free state by removing the partition. The erasure dissipates the heat of $k_BT \ln 2$ (Landauer's bound [9]) by pushing it towards R and exerting the work: $W = \int_1^{0.5} Fd(1-x) = \int_1^{0.5} PAd(1-x) = -\int_1^{0.5} \frac{PAx}{x} dx = -\int_1^{0.5} \frac{k_BT}{x} dx = k_BT \ln 2$. If it is a bit of orientation-encoded classical information, then we still need to input a certain amount of energy above Landauer's bound to reach the designated erasure state from the random data state [8] since the orientation fluctuates and may take an arbitrary direction due to thermal agitation [16].

Since 2012, Landauer's bound has been experimentally verified for various information carriers, including a single silica glass bead [19], a fluorescent particle [20], a single-domain nanomagnet [21], a single atom [22], a giant spin [7], and bacterial ion channels [23], as summarized in Table 2.

Specifically, the sizes of various information carriers and the experimental temperatures are listed in Table 2. Normally, quantum effects are observed at low temperatures and small sizes. For example, when the size of a magnetic particle decreases, it may be possible to invert the magnetization through the quantum tunnelling effect [8]. This effect should appear at low temperatures, where it provides an efficient path for magnetic relaxation only if the wavefunction of the left well overlaps with that of the right well.

Table 2. Experiments on Landauer's bound [9].

Year	Details (Information Carrier)	Size	T(K)	Mode	Violate?
1961	Landauer [9]			Classical	
2012	Silica glass bead [19]	$2 \mu m$	300	Classical	No
2014	Fluorescent particle [20]	200 nm	300	Classical	No
2016	Single-domain nanomagnet [21]	10 ⁴ spins	300-400	Classical	No
2018	Single-atom [22]	⁴⁰ Ca⁺	15 μ	Quantum	No
2018	Giant spin [8]	20 spins	1	Quantum	No
2020	Bacterial ion channels [23]	>> spin	300	Classical	No
2022	Single spin [7][16]	1 spin	1 m	Quantum	Yes

Noticeably, although quantum spin tunnelling was used, the $(20 \ \mu_B)$ giant spin did not break Landauer's bound (i.e., within the experimental uncertainty, the work required for erasure of each giant spin qubit was equivalent to the theoretical Landauer limit $(k_B T \ln 2 \approx 1 \times 10^{-23} J)$ at the experimental temperature of 1 K [8]). This is because, as listed in Table 1, the strength $(\sim 0.1 \ T)$ of the horizontal magnetic field required to overcome the strong magnetic anisotropy in the giant spin reversal experiment [8] is 10^{12} times the magnetic interaction $(10^{-13} \ T)$ in the spin-spin experiment [7]. The detailed calculation follows.

As shown in Figure 6 (top, bottom right), it is the horizontal magnetic field H_z that switches the giant spin (in the same way as how we switch a single spin in Figure 3). As shown in Figure 6 (bottom, left), the transverse magnetic field H_y only plays an assisting role (lowering the barrier) without directly switching the giant spin (although $|H_y| \gg |H_z|$). In theory, a magnetic field that is orthogonal to the easy axis does not contribute to the work required to switch a magnetic moment from one direction along the easy axis to the opposite direction along the same easy axis. In practice, according to the giant spin reversal experiment [8], the measured work done by H_y was $(-6 \pm 2) \times 10^{-24} J$ per molecule, much smaller than the work $[(1.7 \pm 0.3) \times 10^{-23} J$ per molecule] done by H_z . In our study, it suffices to ignore the contribution from H_y .

Thus, the work required for erasure of each $(20\mu_B)$ giant spin qubit can be estimated by a simple formula: $\Delta E_{\uparrow\downarrow}^{20\mu_B} = (20\mu_B)H_z = (20\times9.274\times10^{-24}\,J\cdot T^{-1})\times0.1\,T = 1.855\times10^{-23}\,J$. This estimation reasonably agrees with the experimentally measured total work $((1.1\pm0.3)\times10^{-23}J)$ per molecule) contributed by both H_V and H_Z [8].

It was experimentally verified that the formula $\Delta E_{\uparrow\downarrow}^{N\mu_B} = N\mu_B B$ is universal for calculating the energy required to erase a spin qubit, regardless of whether the information carrier is a single spin or a collective spin (containing N Bohr magnetons). This is important (e.g., the size N of an information carrier matters, although it is not a dominant factor) in terms of implementing quantum computing in spintronics, in which the formula $k_B T$ ln 2 introduced by Landauer in 1961 [9] may not be directly used for the following reason.

Energy well below k_BT ln 2 to erase a qubit at the expense of a long spin relaxation time is theoretically sensible and experimentally verified [7][16]. A single spin extracted from the aforementioned spin-spin magnetic interaction experiment [7] demonstrates that Landauer's bound can be quantitatively broken by a factor of $10^4 \sim 10^{10}$ [16] via quantum spin tunnelling (Figure 10).

The upper bound (10^{10}) of this factor was calculated based on the magnetic field applied by a spin across a distance of 2.76 μ m [16]. The lower bound (10⁴) was calculated based on a Rabi frequency of kHz [16]. By coincidence, as listed in Table 1, the calculated energy ($\sim 10^{-30}$ J) based on the Rabi flopping (Figure 3) reasonably agrees with the energy $(\sim 10^{-30} J)$ of flipping a spin (by pulsing a resonant oscillating magnetic field with the Rabi frequency) in the equivalent magnetic field acting on the spin due to the spinorbit coupling (Figure 5). This coincidence may imply that the single spin system, in which a spin is weakly bound in an ion, is superior by nature to the giant spin (molecular nanomagnet) system, in which a strong anisotropy is inevitably present due to the spin-lattice coupling. Although both the giant spin and single spin use quantum spin tunnelling, the latter is much more 'agile' than the former in terms of the energy required to flip it. Note that the 'clumsiness' of the giant spin is not only due to its 'giant'

size $(20\mu_B)$ but also due to its strong interaction $(10^{12}$ times the spin-spin magnetic interaction) with the surroundings.

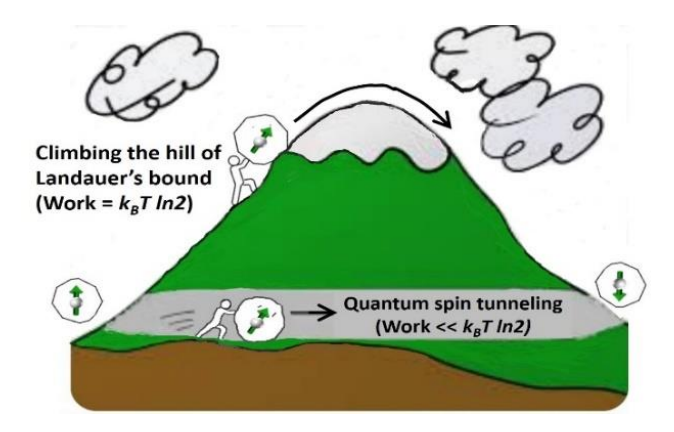


Figure 10. Quantum spin tunnelling penetrates the thermal energy barrier (Landauer's bound [9]) and provides a "shortcut" for spin reversal, which is dramatically different from classical information manipulation (Figure 9). The cost of erasing a spin qubit does not come from "climbing the hill", but from "tunnelling through the hill". Quantum mechanics provides a simple answer to the question of whether it is possible to break Landauer's bound in the envisaged extreme regimes.

This spin tunnelling effect to facilitate reversal of a qubit in quantum computing can be further analysed by rewriting the giant spin Hamiltonian in Equation 1 as:

$$\mathcal{H} = -D_{ani}S_z^2 + E_{ani}(S_x^2 - S_y^2) - 2\mu_B S_x \cdot H_x - 2\mu_B S_y \cdot H_y - 2\mu_B S_z \cdot H_z.$$
 (10)

If $H_x = 0$ and $H_y = 0$ (as mentioned above, the transverse magnetic fields do not directly switch a magnetic moment), then the eigenvectors of this Hamiltonian are the eigenvectors $|m\rangle$ of S_z and the eigenvalues of this Hamiltonian are therefore quantized and equal to

$$E_m = -D_{ani}m^2 - 2\mu_B m H_z, \tag{11}$$

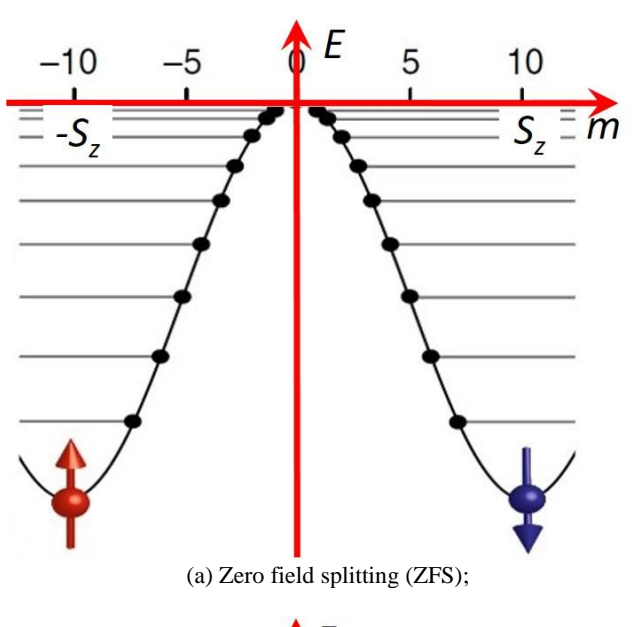
where s designates the eigenvalues of the spin operator S_z and $m = -S_z$, $-(S_z - 1)$, $-(S_z - 2)$, ..., $(S_z - 1)$, S_z . Thus, there are $(2S_z+1)$ eigenvectors and $(2S_z+1)$ eigenvalues.

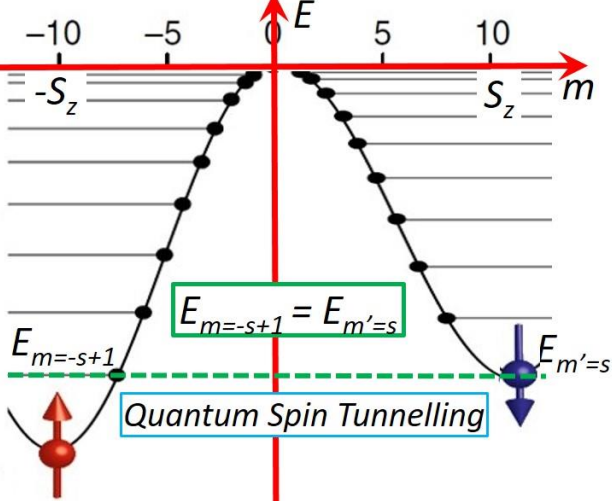
If $H_z = 0$, then the eigenvectors $|m\rangle$ and $|-m\rangle$ are degenerate as shown in Figure 11(a), in which splitting of the (2S+1) energy levels can be seen even in the absence of an applied magnetic field (zero-field splitting, ZFS) [24]. If $H_z \neq 0$, then it is possible to have degeneracy $(E_m = E_{m'})$ of two eigenvectors $|m\rangle$ and $|m'\rangle$ for certain values of H_z [24]. As an example, Figure 11(b) shows the level in the double well when $E_{m=-s+1} = E_{m'=s}$ is satisfied. That is, tunnelling is triggered (with the assistance of an appropriate transverse field H_x or H_y) between the lowest (ground) state of the right-hand well and the first excited state of the left-hand well.

According to the Arrhenius law [24], a 'potential barrier' is present in the form of Landauer's bound k_BT [9]:

$$k_B T_0 = |D_{ani}| s^2 - \frac{|D|}{4},\tag{12}$$

where *s* is a half-integer (it becomes $k_BT_0 = |D_{ani}|s^2$ for an integer spin) and the anisotropy constant D_{ani} may be negative. In other words, the energy landscape is a parabola $(\propto S_z^2)$ whose maximum at $S_z = 0$ is a potential barrier [24], as shown in Figure 11(a). Note that the maximum appears at $S_z \neq 0$ in Figure 11(b), where $H_z \neq 0$.





(b) subject to a longitudinal magnetic field.

Figure 11. Energy levels of a (giant) spin. (a) Zero field splitting (ZFS); (b) subject to a longitudinal magnetic field that satisfies $E_{m=-s+1} = E_{m'=s}$. Tunnelling is triggered (with the assistance of an appropriate transverse field) between the lowest (ground) state of the right-hand well and the first excited state of the left-hand well.

Physically, a spin qubit is a quantum and it takes the time Δt with the spread in energy ($\Delta E = {^\hbar/_{\Delta t}}$, where $\hbar \approx 10^{-34} \, J \cdot s$ is the reduced Planck constant) to flip according to Heisenberg's time-energy uncertainty relation [5][18]. If a slow erasure (typically, $\geq 100 \, s$) is operated, then the consumed energy ($\Delta E \approx 10^{-36} \, J$) is 10^{-10} times Landauer's bound [16]. Here, it is the quantum limit ($10^{-34} \, J \cdot s$), rather than Landauer's bound, that governs the performance of a spin qubit [7][16]. Among the various information carriers listed in Table 2, a single spin is the smallest and the closest to the quantum limit [5][16].

As a matter of fact, Landauer's bound has already been significantly challenged over the past two decades [25]. In 2000, Shenker argued that it is plain wrong since logical irreversibility is unrelated to heat dissipation [26]. In 2003, Bennett suggested that it is a restatement of the second law of thermodynamics [27]. In 2011 and 2019, Norton showed that the thermal fluctuation selectively neglected in the previous proofs fatally disrupted the intended operation [28][29].

In addition to these theoretical arguments [25-29], strong experimental evidence [7][16] has already demonstrated that Landauer's bound is no longer the smallest amount of energy for erasing a spin qubit. We may therefore have to presume the demise of the bound despite the many mysteries uncovered with it over the past 60 years [30].

A large cooling facility that is peripheral to the central quantum processor is needed for today's few-qubit quantum computers, in which the fundamental energy given by $\Delta E = \mu_B B$ merely represents a small part of the overall energy bill. However, the cooling energy is unlikely to scale linearly with the increased number of qubits [22]; hence, its relative proportion will become less dominant in the future.

V. Energy-Efficient Adiabatic Quantum Computer

The above spin-encoded quantum computer may be slow although it can operate at the ultimate (energy) limit for computation set by physics. Amazingly, such a slow operation or slow evolution is good for adiabatic quantum computing [31][32][33].

If the Hamiltonian of a quantum computer depends on time, then its quantum state vector should satisfy the equation

$$i\hbar \frac{d|\Psi(t)\rangle}{dt} = \widehat{H}(t)|\Psi(t)\rangle. \tag{13}$$

At a given time, the Hamiltonian will have a set instantaneous eigenvectors, such that $\widehat{H}(t)|\Psi_n(t)\rangle = E_n(t)|\Psi_n(t)\rangle$. For example, its ground state will also be time dependent.

In adiabatic quantum computing, we need to find a (potentially complicated) Hamiltonian whose ground state describes the solution to our problem of interest. First, we initialise our system with a simple Hamiltonian to the ground state (i.e., $|\Psi(0)\rangle = |\Psi_g(0)\rangle$). Next, we let the simple Hamiltonian evolve to the desired complicated Hamiltonian in an adiabatic way [the ground state of our system is always

separated from the excited states by a finite energy gap (i.e., $E_1(t) - E_0(t) > 0$)]. By the adiabatic theorem [1], if the Hamiltonian evolves slowly enough to avoid the metastable states (none of which is close to our solution), then our system remains in the ground state (i.e., $|\Psi(t)\rangle = |\Psi_0(t)\rangle$, and the final state of our system encodes the solution to our problem in one go (evolution).

The adiabatic evolution in the case of a single spin qubit can be explained as follows. The Hamiltonian

$$\widehat{H}(t) = -\frac{1}{2} \begin{pmatrix} \varepsilon(t) & \Delta \\ \Delta & -\epsilon(t) \end{pmatrix} \tag{14}$$

depends on time through the bias ε . Its ground state is $\left|\Psi_g\left(-\infty\right)\right\rangle = \begin{pmatrix} 0\\1 \end{pmatrix}$ (i.e., in the $\left|\downarrow\right\rangle$ potential well) when $\varepsilon = -\infty$ and $\left|\Psi_g\left(\infty\right)\right\rangle = \begin{pmatrix} 1\\0 \end{pmatrix}$ ($\left|\uparrow\right\rangle$ potential well) when $\varepsilon = \infty$.

As shown in Figure 12, if the qubit is initially in the ground state and the bias then slowly changes from minus to plus infinity, then the qubit will have time to tunnel from the $|\downarrow\rangle$ to $|\uparrow\rangle$ potential well, and will end up in the ground state. If the evolution is too fast by rapidly changing the bias, then the qubit will remain trapped in the $|\downarrow\rangle$ potential well, that is, in the excited state. This 'trapping' is a major source of error in adiabatic quantum computing [1][31][32][33].

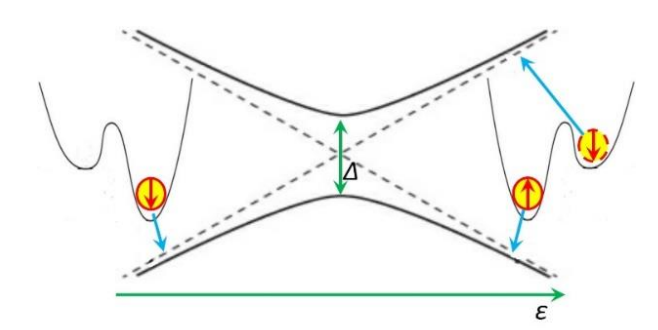


Figure 12. Slow evolution of a spin qubit in adiabatic quantum computing operating at the ultimate energy limit. If the evolution is too fast, then the qubit will jump from the ground state to the excited state by mistake.

The adiabatic quantum computer has some obvious advantages: any quantum program can be run on it; the quantum gates can be replaced by qubit-qubit interactions; there is no need to precisely manipulate the states of qubits; and the ground state is the lowest energy state [1]. Therefore, as long as we run the system slowly and keep the ambient temperature lower than the energy gap between the excited state and the ground state, we can suppress the noise coming from the outside and preserve the required quantum coherence for a long time.

VI. Conclusion

In this study, we compared two typical spintronic systems in terms of using spins as qubits: one is a giant spin (molecular nanomagnet) with strong anisotropy due to the spin-lattice coupling [8]; the other is a single spin that is weakly bound in an ion [7][34]. We found that although both use quantum spin tunnelling, the single spin is much more 'agile' than the giant spin (whose 'clumsiness' is not only due to its 'giant' size but also due to its strong coupling with the surroundings) and can break Landauer's bound (the energy of erasing a classical bit of information) by a factor of $10^4 \sim 10^{10}$. Experimental verification is provided, in which the single spin is optically manipulated by a circularly polarized onresonant laser (with a wavelength ranging from 422 nm to 1092 nm) and Rabi flopping at mHz [7]. Our theory showed that the quantum dynamics of a spin qubit are largely determined by its energy-time product. We also demonstrated that the slow evolution of a spin qubit that is operated at the ultimate energy limit is good for adiabatic quantum computing.

In conclusion, quantum spintronics (with a single spin as a qubit) may represent a new energy-efficient sub-Landauer-bound computing paradigm. According to Koomey's law [35][36], Landauer's bound limits irreversible operations such that the increase in the computing power efficiency (the number of computations per joule of energy dissipated) will come to a halt around 2050.

REFERENCES

- [1] A. Zagoskin, Quantum Mechanics: A Complete Introduction: Teach Yourself. John Murray Press. 2015.
- [2] U. Banin, Y. Cao, D. Katz, O. Millo, "Identification of atomiclike electronic states in indium arsenide nanocrystal quantum dots", Nature, 400, 1999.
- [3] Y. Nakamura, Y. Pashkin & J. Tsai, "Coherent control of macroscopic quantum states in a single-Cooper-pair box", Nature, 398, 1999.
- [4] B. D. Josephson, "Possible new effects in superconductive tunnelling". Phys. Lett. 1 (7): 251–253, 1962.
- [5] R. Feynman, R. Leighton and M. Sands, Feynman Lectures on Physics, Vols I, II and III. Basic Books, 2010.
- [6] L. Vandersypen, M. Steffen, G. Breyta, et al., "Experimental realization of Shor's quantum factoring algorithm using nuclear magnetic resonance", Nature 414, 2001.
- [7] S. Kotler, et al. "Measurement of the Magnetic Interaction Between Two Bound Electrons of Two Separate Ions", Nature, V.510, I.7505, 2014.
- [8] R. Gaudenzi, et al. "Quantum Landauer erasure with a molecular nanomagnet", Nature Physics, 14 (6): 565–568, 2018.
- [9] R. Landauer, "Irreversibility and Heat Generation in the Computing Process", IBM J. Res. Develop. 5, 183–191, 1961.
- [10] S. Haroche, "Quantum beats and time-resolved fluorescence spectroscopy", High-Resolution Laser Spectroscopy, Topics in Applied Physics, Vol. 13, Springer Berlin Heidelberg, 1976.
- [11] Michael Irving, Astronomers detect strongest known magnetic field in the universe, https://newatlas.com/space/strongest-magnetic-field-detected/, September 10, 2020.
- [12] China claims new world record for strongest steady magnetic field, https://www.eurekalert.org/news-releases/961695, News Release 12-Aug-2022.
- [13] N. Savage, "The world's most powerful MRI takes shape", IEEE Spectrum, Vol.50, No.11, pp. 1112, Nov. 2013.

- [14] A Modern Well-Designed 60 Hz Power Transformer Will Probably Have a Magnetic Flux Density Between 1 and 2 T Inside the Core. https://eece.ksu.edu, Apr. 17, 2021.
- [15] Orders of Magnitude (Magnetic Field), https://en.wikipedia.org/wiki/Orders_of_magnitude, accessed 08 January 2023.
- [16] F. Wang, "Breaking Landauer's Bound In A Spin-Encoded Quantum Computer", Quantum Information Processing, Springer Nature, 21:378, 2022.
- [17] J. Thompson, Scientists just broke the record for the coldest temperature ever recorded in a lab, https://www.livescience.com/coldest-temperature-ever, October 14, 2021.
- [18] S. Lloyd, "Ultimate physical limits to computation", Nature, VOL 406, 31 August 2000.
- [19] A. Bérut, et al. "Experimental Verification of Landauer's Principle Linking Information and Thermodynamics", Nature, 483-187, 2012.
- [20] Y. Jun, et al. "High-Precision Test of Landauer's Principle in a Feedback Trap", Physical Review Letters, 113 (19): 190601, 2014.
- [21] J. Hong, et al. "Experimental test of Landauer's principle in single-bit operations on nanomagnetic memory bits". Science Adv.. 2 (3), 2016.
- [22] L. L. Yan, T. P. Xiong, K. Rehan, F. Zhou, D. F. Liang, L. Chen, J. Q. Zhang, W. L. Yang, Z. H. Ma, and M. Feng, "Single-Atom Demonstration of the Quantum Landauer Principle" Phys. Rev. Lett. 120, 210601, 2018.
- [23] U. Çetiner, O. Raz, S. Sukharev, "Dissipation During the Gating Cycle of the Bacterial Mechanosensitive Ion Channel Approaches the Landauer's Limit", doi: https://doi.org/10.1101/2020.06.26.174649, 2020.
- [24] D. Gatteschi, R. Sessoli, J. Villain, Molecular Nanomagnets Vol. 5 (Oxford Univ. Press, Oxford, 2006).
- [25] https://en.wikipedia.org/wiki/Landauer%27s_principle, accessed 08 January 2023.
- [26] O. Shenker, Logic and Entropy, http://philsci-archive.pitt.edu, 2000
- [27] C. Bennett, "Notes on Landauer's principle, reversible computation, and Maxwell's Demon", Stud. Hist. Philos. Mod. Phys., vol. 34, pp. 501-510, 2003.
- [28] J. D. Norton, "Waiting for Landauer", Studies in History and Philosophy of Modern Physics, 42, pp.184-198, 2011.
- [29] J. Norton, A Hot Mess: Author's Response, https://sites.pitt.edu/~jdnorton/papers/Hot_mess_Response.pdf , 2019.
- [30] I. Georgescu, "60 years of Landauer's principle", Nature R. P., 17/11, 2021.
- [31] E. Farhi, J. Goldstone, S. Gutmann, M. Sipser, "Quantum Computation by Adiabatic Evolution". arXiv:quantph/0001106v1, 2001.
- [32] T. Kadowaki, H. Nishimori, "Quantum annealing in the transverse Ising model". Physical Review E. 58 (5): 5355. arXiv:cond-mat/9804280, 1998.
- [33] A. Finilla, M. Gomez, C. Sebenik, D. Doll, "Quantum annealing: A new method for minimizing multidimensional functions". Chemical Physics Letters. 219 (5): 343–348. arXiv:chem-ph/9404003, 1994.
- [34] F. Wang, "Can We Break the Landauer Bound in Spin-Based Electronics?", IEEE Access. 67109-67116, 2021.
- [35] J. Koomey, S. Berard, M. Sanchez, H. Wong, "Implications of Historical Trends in the Electrical Efficiency of Computing", IEEE Annals of the History of Computing, 33 (3): 46–54, 2010.

[36] J. Koomey, "Our latest on energy efficiency of computing over time, now out in Electronic Design", 29 November 2016.